Hindawi
Journal of Nanotechnology
Volume 2017, Article ID 2791282, 9 pages
https://doi.org/10.1155/2017/2791282

Research Article

Fabrication of Fiber Bragg Grating Coating with TiO_2 Nanostructured Metal Oxide for Refractive Index Sensor

Shaymaa Riyadh Tahhan,[1] Rong Zhang Chen,[2] Sheng Huang,[2] Khalil I. Hajim,[3] and Kevin P. Chen[2]

[1]*Laser and Optoelectronics Engineering Department, College of Engineering, Nahrain University, Al-Jadriya, Baghdad, Iraq*
[2]*Department of Electrical and Computer Engineering, University of Pittsburgh, Pittsburgh, PA, USA*
[3]*Dijlah University, Baghdad, Iraq*

Correspondence should be addressed to Shaymaa Riyadh Tahhan; shaymaa.riyadh@gmail.com

Received 1 October 2016; Accepted 4 January 2017; Published 16 March 2017

Academic Editor: Baofu Ding

To increase the sensitivity of biosensor a new approach using an optical fiber Bragg grating (FBG) coated with a suitable nanostructured metal oxide (NMO) is proposed which is costly effective compared to other biosensors. Bragg grating was written on a D-shaped optical fiber by phase mask method using a 248 nm KrF excimer laser for a 5 min exposure time producing a grating with a period of 528 nm. Titanium dioxide (TiO_2) nanostructured metal oxide was coated over the fiber for the purpose of increasing its sensing area. The etched D-shaped FBG was then coated with 312 nm thick TiO_2 nanostructured layer to ensure propagating the radiation modes within the core. The final structure was used to sense deionized water and saline. The etched D-shaped FBG original sensitivity before coating to air-deionized water and to air-saline was 0.314 nm/riu and 0.142 nm/riu, respectively. After coating the sensitivity became 1.257 nm/riu for air-deionized water and 0.857 nm/riu for air-saline.

1. Introduction

Swanton et al. in 1996 used the phase mask method to write uniform photorefractive FBG [1]. To enhance the written FBGs, high pressure hydrogen gas (H_2) was loaded in the optical fiber to increase the UV photosensitivity before writing the grating [2]. A novel approach of designing a chemosensor, based on cladding etched Bragg grating, was reported by Zhou et al. in 2004, where the FBG sensitivity to the refractive index of surrounding medium increases by HF etching. A measured sensitivity of 0.02 nm/% was obtained for different sugar solution concentrations [3]. FBG was coated with different thicknesses of SiO_2 nanoparticle mesoporous thin films and used as a refractive index sensor. This sensor showed a high sensitivity of 1927 nm/riu to RI changes with a response time shorter than 2 sec [4]. Specific and highly sensitive chemical sensors for in-water monitoring were made by coating fiber long period gratings with a nanoscale Syndiotactic Polystyrene (sPS) in nanoporous crystalline form by dip coating technique [5]. Other methods of coating were used to fabricate an optical chemical sensor in which the etched region of FBG was coated by a thin layer of gold nanoparticles to detect and determine the manganese concentration in water [6]. FBG was coated with different film thicknesses of gold by sputtering deposition technique and using it as a chemical sensor for ethanol in aqueous solution. It was found that the 50 nm gold film enhances the evanescent wave on the optical fiber surface and increases its sensitivity to detect ethanol with different concentrations [7].

Mantzila and Prodromidis in 2005 [8] anodically formed films of titanium oxide at 0.5–65 V in 1 M H_2SO_4 for 1 h under mild stirring. The films were characterized by electrochemical impedance spectroscopy, scanning electron microscopy, Raman spectroscopy, ellipsometry, and diffuse reflectance FT-IR spectroscopy.

Davies et al. in 2008 [11] were the first to investigate the sol-gel coated FBG for refractive index sensors. The sol-gel was made from titanium and silicon oxide coatings. The

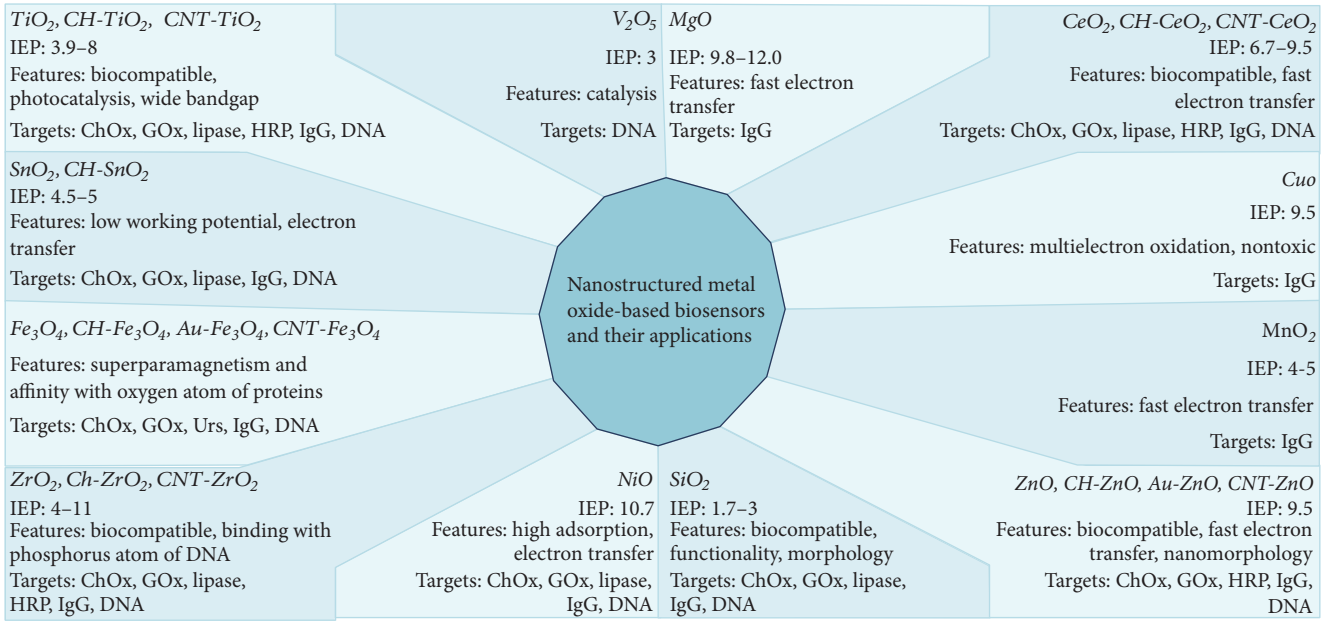

Figure 1: Nanostructured metal oxide-based biosensors and their applications (IEP, isoelectric point; ChOx, cholesterol oxidase; GOx, glucose oxidase; HRP, horseradish peroxidase; IgG, Immunoglobulin G; Urs, urease) [9].

results revealed a refractive index sensitivity dependence on thickness and index of the coating. The sensitivity of the coated FBG was higher than the uncoated region.

In 2010, Mun et al. [12] stated that optical interferometry of TiO_2 thin film array of nanotubes allows label free sensing of rabbit immunoglobulin G (IgG) by using protein A as a capture probe, immobilized on the nanotubes inner pore walls by electrostatic adsorption.

Liang et al. in 2011 [13] proved that the FBG sensitivity is based on the effective index for the waveguided mode. This sensitivity depends on the refractive index change of the ambient medium and the Bragg wavelength shift.

In the same year, Smietana et al. [14] presented the temperature sensing properties of a silicon nitride (SiNx) nanocoated long period grating. The SiNx nanocoating was applied to tune the external refractive index sensitivity of LPG, written with UV and electric arc technique. This work presented for the first time a nanocoating capable of simultaneously tuning the RI sensitivity and enabling temperature measurements in high-RI liquids applied to LPGs.

In 2012, Chen [15] studied and used the FBG sensors for extreme environments. They also used the KrF excimer laser to write the FBG by the phase mask method.

In 2013, Zhang et al. [16] coated the FBG with a bimaterial microscale using laser assisted maskless microdeposition and electroless nickel plating. Bimaterial coating enhanced the sensitivity of the FBG; the temperature sensitivity was doubled as compared to bare FBG.

In the same year, Ho et al. [17] designed a FBG sensor to detect the presence of the water entering concrete structures after being cracked by environmental effects. This work represents the first experiment tested the repeatability of the sensor to cyclic input of various volumes of water, and it tested the sensor's response to flooding conditions. The sensor had a good repeatability with fast response time <10 min.

The present work is concerned with the study of the performance of FBG coated with NMO materials to sense biomaterials. The main purpose of this research using the TiO_2-NMO with FBG is to enhance its sensitivity feature reaching to the sensing of so many diseases which cannot be detected conventionally.

The prepared FBG coated with TiO_2 NMO (20 nm holes diameter) may be used in antibody sensing if we use the protein type A (5 nm diameter) to fill the pores of the TiO_2 NMO and then bind with the antibody type IgG1 and IgG2 leading to highly likely related Bragg shift corresponding to expected variation in the effective index.

The main interest is to prepare cost effective, small size, and less cumbersome biosensor. Large sensing area of FBG coated with NMO is our proposed biosensor.

2. Theoretical Background

2.1. Nanostructure Metal Oxide. NMO materials have great potential as immobilizing matrices for biosensor development [9]. Their use may lead to the fabrication of novel biosensor devices needed to enhance diagnostic. Bruggmann Effective Medium was employed to calculate the effective index of the NMO with the biological liquids or tissues (solid-liquid into and nanobiointerfaces) to fabricate an efficient biosensor. Figure 1 shows many types of NMOs and their biosensing applications [9].

2.2. Bruggmann's Effective Medium Theory. Metal oxide nanostructure material is a composite material with effective index worked out by Bruggmann's effective medium theory

[10, 18]. Bruggmann's approximation starts from Clausius-Mossotti Approximation and involves knowing if a polarizable entity is a sphere of dielectric constant ε_1 and radius a. If so, then elementary electrostatics polarizability is given by [18]

$$\alpha = \frac{(\varepsilon_1 - 1)\, a^3}{(\varepsilon_1 + 2)}, \tag{1}$$

where α is the polarizability.

Substituting the above equation in the following equation:

$$\frac{(\varepsilon - 1)}{(\varepsilon + 2)} = \frac{(4\pi n\alpha)}{3} \tag{2}$$

it yields

$$\frac{\varepsilon - 1}{\varepsilon + 2} = \eta_1 \frac{\varepsilon_1 - 1}{\varepsilon_1 + 2}, \tag{3}$$

where ε is the effective dielectric constant; η_1 is the fraction of space occupied by material with dielectric constant ε_1.

The embedded sphere in a material of dielectric constant ε_0 is then replaced as follows:

$$\frac{\varepsilon - \varepsilon_0}{\varepsilon + 2\varepsilon_0} = \eta_1 \frac{\varepsilon_1 - \varepsilon_0}{\varepsilon_1 + 2\varepsilon_0}. \tag{4}$$

Equation (4) was derived originally from the following equation:

$$\varepsilon - 1 = \frac{4\pi n\alpha E_{\text{eff}}}{E} = \frac{4\pi n\alpha\,(E + 4\pi P/3)}{E} = 4\pi n\alpha \frac{\varepsilon + 2}{3}, \tag{5}$$

where E_{eff} is the effective field as follows [18]:

$$E_{\text{eff}} = E + \left(\frac{4}{3}\right)\pi P, \tag{6}$$

where E is the space average field, P is the polarization which is equal to (np), where n is the number of polarizable entities per unit volume, and p is the induced dipole moment of each.

Bruggmann found that the total polarization summed over the two types of inclusion must vanish; thus,

$$\delta_1 \frac{\sigma_1 - \sigma_m}{\sigma_1 + 2\sigma_m} + \delta_2 \frac{\sigma_2 - \sigma_m}{\sigma_2 + 2\sigma_m} = 0, \tag{7}$$

where σ_1 is the first material conductivity, σ_m is the effective conductivity, σ_2 is the second material conductivity, δ_1 is the first material fraction volume, and δ_2 is the second material fraction volume, $\delta_1 + \delta_2 = 100\%$ or 1. This approximation is the mostly acceptable in this field [18].

3. Tools and Methods

A fiber was coated by a nanostructured TiO_2 followed and then tested by injecting it in some liquids. The procedure is explained in Figure 2.

3D nanostructures TiO_2 were papered by Sol-Gel method, using the following chemicals: Ethanol (CH_3CH_2OH), 7.5 gram

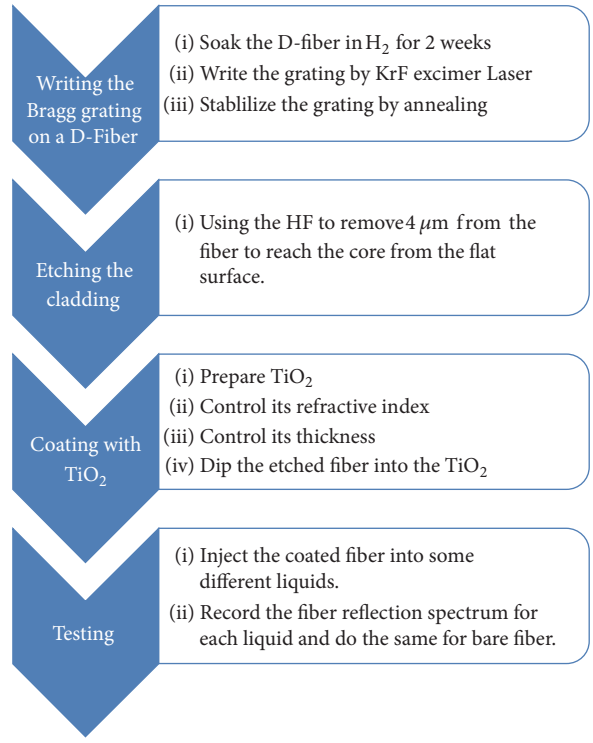

Figure 2: Procedure structure.

(i) Titanium tetrachloride ($TiCl_4$), 0.48 gram

(ii) Hydrochloric acid (HCl), 1.18 gram

(iii) Pluronic-F127, 0.5 gram

Ethanol was mixed, using a stirrer, with drop by drop addition of $TiCl_4$. The weight measurement was continuously taken during mixing. The solution was left at room temperature for a while until reaching ambient temperature. 0.5 gm of Pluronic F-127 was added to the solution while stirring. Hydrochloric acid (HCL) was then added slowly, 2 drops per 30 min, while stirring till the solution turned clear. The PH of the solution was adjusted to 0.5 during stirring and HCl addition. Finally, the solution was stirred for three hours and finally left to set for 24 hours.

3.1. Refractive Index Measurement. 1 cm by 1 cm Thermal Oxide wafer [300 nm SiO_2 layer on Si ($n = 1.455$)] was spin-coated by coater (Headway Research Inc.) with TiO_2 sol-gel. The prepared wafer was placed in a furnace to dry for 2 hours at 60°C. The temperature was made to increase at 3°C/min rate until reaching 120°C and stayed there an hour. Special temperature controller was utilized for this purpose which at the end reached 600°C and held there for 2 hours. Finally, the temperature was decreased by 3°C/min rate until reaching the room temperature at 25°C. Figure 3 shows schematically how the furnace program is run.

To measure the refractive index of the prepared TiO_2 NMO over the wafer, a spectroscopic ellipsometry (HORIBA JOBIN YVOIN) was employed.

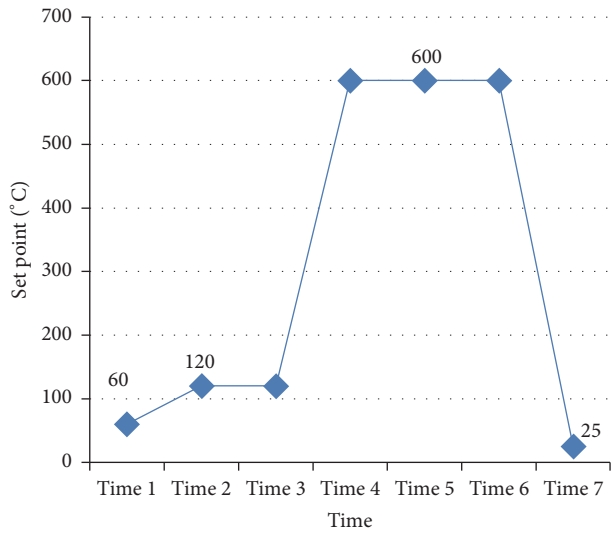

Figure 3: Schematic presentation of the controlled furnace temperature.

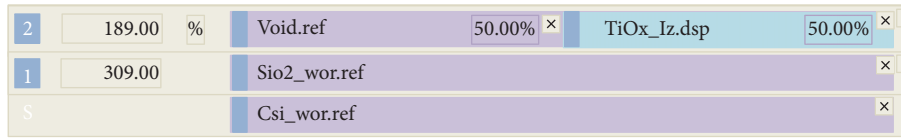

Figure 4: Fitting procedure for the wafer films coated with NMO-TiO_2.

Table 1: Different concentrations of sol-gel preparation for thickness measurements.

Ethanol (g)	$TiCl_4$ (g)	F-127 (g)	HCl (g)
4.5	0.48	0.5	0.7
7.5	0.48	0.5	1.18
9.5	0.48	0.5	1.4
10.5	0.48	0.5	1.42

The samples were fitted as shown in Figure 4, where the wafer film is Si with a 300 nm of SiO_2. This wafer is coated with porous TiO_2 and the third layer is TiO_2 with voids. The voids represent air porosity. The angle of incidence was 70° and the spectrum range is from 400 to 1600 nm by 10 nm increment. The obtained data is shown in Figure 5.

3.2. Thickness Control. Four different TiO_2 Sol-Gels were prepared with different concentrations (Table 1) as a preliminary study to find the suitable thickness over the fiber.

The preparation details are presented in Section 3.1 (TiO_2 NMO preparation method). The 4–6 cm long D-shaped fiber jacket was removed by a fiber-optic stripper and then cleaned by tissue with some ethanol. The D-shaped fiber was dipped into the TiO_2 sol-gel for 20–30 seconds and then dried in the furnace, as explained in Refractive Index Measurement.

JEOL USA JSM-6510LV Scanning Electron Microscope was utilized to measure the thickness of the NMO material on the fiber. Picturing the fiber samples necessitated coating with conducting Palladium ions using CRESSINGTON 108 autosputter coater.

3.2.1. Coating Process. The etched D-shaped fiber was exposed to TiO_2 sol-gel by drawing the fiber at 5 mm/s rate. The fiber was then dried for one day in air and then placed in a furnace following the same program mentioned in Refractive Index Measurement.

Testing the Fabricated FBG-TiO_2. The sensing assembly consists of five main elements. The FBG-TiO_2 NMO was connected from one end to an optical circulator which was connected to a broadband light source type MPB EBS-7210 with a center wavelength of 1565 nm and spectral width of 100 nm at −20 dBm and to Agilent 86140 series optical spectrum analyzer with a wavelength range of 600 nm to 1700 nm and accuracy of ±0.01 nm for 1480 to 1570 nm. The FBG-TiO_2 NMO was placed in a glass tube; then deionized water and saline were injected into this tube for sensing. The assembly is shown in Figure 6.

The Bragg wavelength was recorded in air, deionized water, and saline. To ensure that the prepared FBG-TiO_2 NMO was better than that without NMO coating, the etched

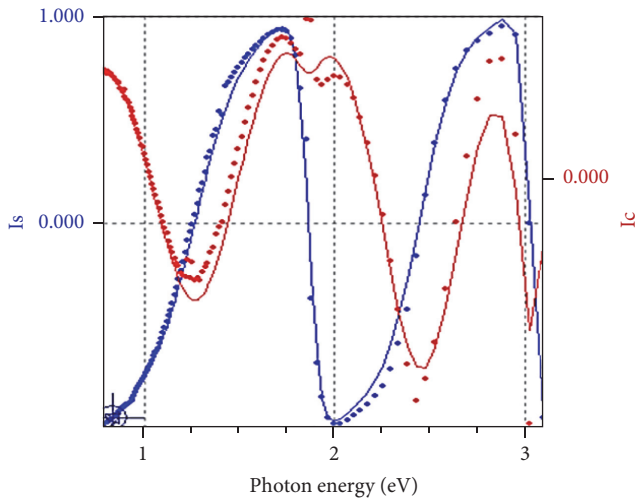

Figure 5: Spectroscopic ellipsometry data fitting procedure of TiO_2 NMO.

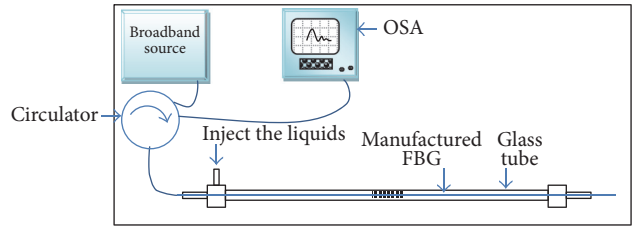

Figure 6: Reflection spectrum measurement by a D-shaped FBG with TiO_2.

D-shaped FBG was used in the same assembly to record the Bragg wavelength for air, deionized water, and saline.

4. Results

4.1. Spectroscopic Ellipsometry Refractive Index Results. The refractive index of the coated TiO_2 NMO on a thin film was measured as a function of the incident wavelengths and found to be 1.487 at 1550 nm, Figure 7.

4.2. Scanning Electron Microscope Thickness Results. The theoretical value of the coated TiO_2 NMO thickness over the D-shaped fiber was deduced from the results published by Poole et al. of which Comsol multiphysics simulation was applied [10, 19]. Their work was done for tin dioxide (SnO_2) as shown in Figure 8. The figure gives a combined refractive index and losses percentage for a given set of thicknesses. In our experiment, the desired 1.6 effective refractive index requires thicknesses that may range between 200 nm and 300 nm taking into account the difference in the optical properties of the TiO_2 and SnO_2. Nevertheless this refractive index does not satisfy the guiding condition of light through the fiber; so a control on the thickness of the coated NMO was needed. This thickness should keep the radiation modes of light beam propagating inside the optical fiber when it is dipped in the postulated solutions.

Many TiO_2 sol-gel samples for coating the fiber were prepared and examined by SEM to find the suitable concentration of the TiO_2 to sense saline.

Figures 9(a) and 9(b) show the SEM images for 4 prepared coated D-shaped optical fibers.

For (9 : 0.96 : 1 : 1.4) g ratio of ethanol : $TiCl_4$: F-127 : HCl of TiO_2 NMO coating over the optical fiber gave a thickness of about 339 nm. The ethanol concentration was increased by 65% of its first value, and the second ethanol : $TiCl_4$: F-127 : HCl (15 : 0.96 : 1 : 2.36) g ratio of TiO_2 NMO coating over the optical fiber gave a thickness of about 312 nm. The ethanol concentration was then increased by 25% of its second value, and the third ethanol : $TiCl_4$: F-127 : HCl (19 : 0.96 : 1 : 2.8) g ratio of TiO_2 NMO coating over the optical fiber gave a thickness of about 244 nm.

The ethanol concentration was finally increased by 10% of its third value, and the fourth ethanol : $TiCl_4$: F-127 : HCl (21 : 0.96 : 1 : 2.84) g ratio of TiO_2 NMO coating over the optical fiber resulted in a thickness of about 207 nm.

Figure 11 shows a relationship between ethanol concentrations and the resultant thickness of the TiO_2 NMO coating over the D-shaped optical fiber. From these results and Figure 9, the best TiO_2 sol-gel concentration was the second one.

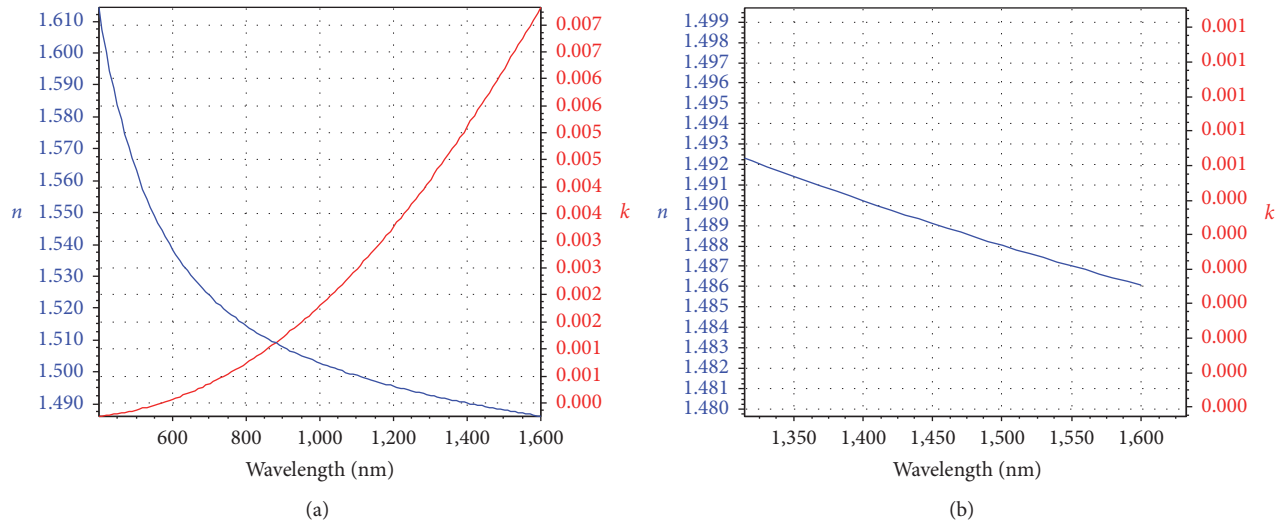

FIGURE 7: (a) The refractive index (real part (n) and imaginary part (k)) of TiO_2 NMO as a function of the incident wavelength as a result from the spectroscopic ellipsometry for the sample prepared in Section 3.1 (TiO_2 NMO preparation method). (b) Magnification of the real part of the refractive index of TiO_2 NMO.

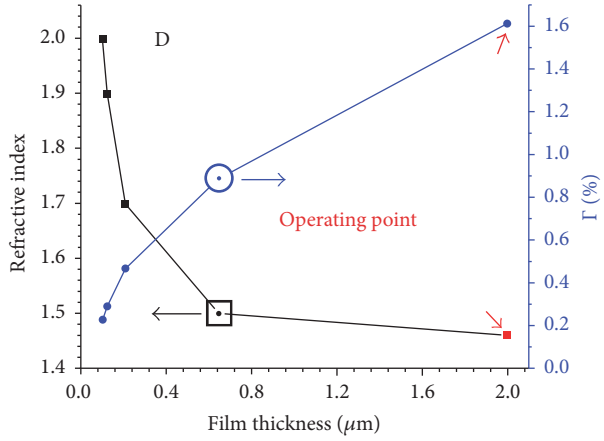

FIGURE 8: The relation between the effective refractive index of NMO-SnO_2 and its thickness on the optical fiber [10].

4.3. Assembly Results with a Bare FBG. The etched D-shaped FBG sensing ability was tested as shown in Figure 9. The reflection spectrum was recorded and presented in Figure 11. The black line refers to the FBG in air and the green line refers to the same sample but dipped in deionized water. It is obvious from this figure that there is a slight shift in the Bragg wavelength due to the difference in refractive index between air ($n = 1$, $\lambda_{Bragg} = 1549.8$ nm) and deionized water ($n = 1.318$, $\lambda_{Bragg} = 1549.9$ nm) so the wavelength shift $\Delta\lambda_{Bragg}$ is 0.1 nm. The sensitivity (ratio between the Bragg wavelength shift and the difference in the surrounding index, $\Delta n_{surrounding} = 0.318$) was deduced and found to be 0.3144 nm/riu.

The deionized water was replaced by saline water. The same measurements were recorded and the resultant reflectivity spectrum was recorded as shown in Figure 12, where the reflection spectrum recorded (the black line) refers to the FBG in air $\lambda_{Bragg} = 1549.8$ nm and the green line refers to the same sample but dipped in saline water $\lambda_{Bragg} = 1549.75$ nm. It is obvious from this figure that there is a very slight shift of 0.05 nm in the Bragg wavelength. The sensitivity was 0.142 nm/riu.

4.4. Assembly Results with FBG-TiO_2 NMO. The etched D-shaped FBG was coated with ethanol : $TiCl_4$: F-127 : HCl at 15 : 0.96 : 1 : 2.36 g ratio of TiO_2 sol-gel and dried at the ambient temperature for 24 hours. The sample was used in the assembly shown in Figure 6 to test its sensing ability. The reflection spectrum was recorded in air as shown in Figure 13 (black line, $\lambda_{Bragg} = 1549.8$ nm). The measurement was repeated after dipping in a deionized water and the resultant

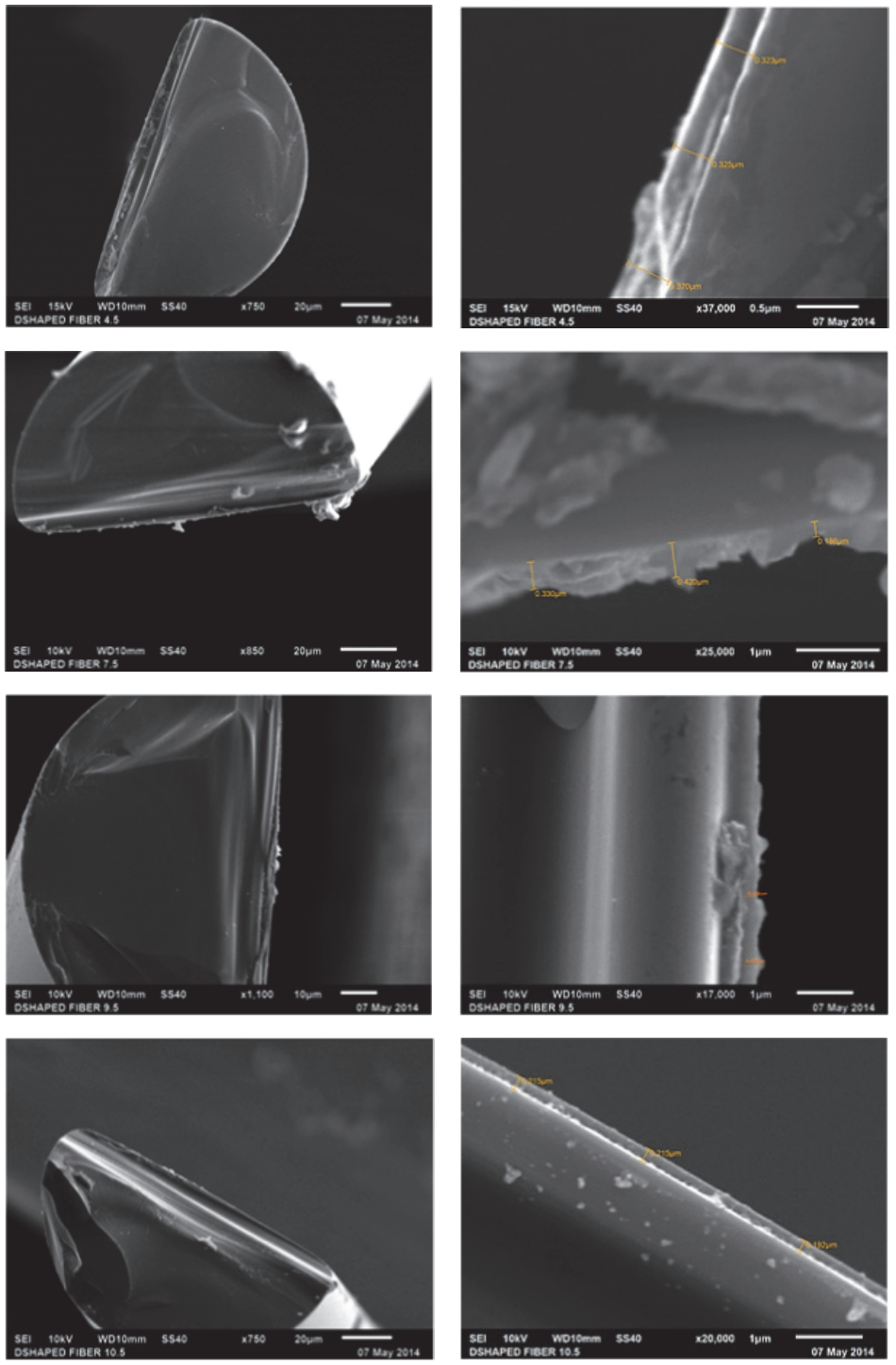

(a) (b)

FIGURE 9: The SEM pictures of the D-shaped fiber coated with nanostructured metal oxide material (TiO_2). (a) is an amplified image of (b). The mean values of the resultant thickness measurement are shown in Figure 10.

reflection spectrum is shown in Figure 13, (green line, λ_{Bragg} = 1549.4 nm). The obtained sensitivity was 1.257 nm/riu.

The deionized water was then replaced by saline water. The same measurements were recorded and the resultant reflectivity spectrum was recorded as shown in Figure 14.

The reflectivity spectrum of the TiO_2 NMO coated FBG in air is in a black line with λ_{Bragg} = 1549.8 nm and the reflectivity spectrum of the same sample but in saline water is in a green line with λ_{Bragg} = 1549.5 nm. The sensitivity is 0.857 nm/riu.

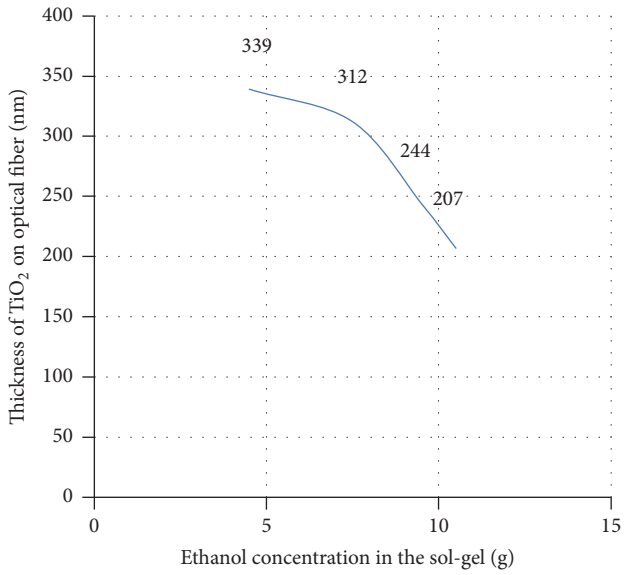

Figure 10: The relation between the different concentrations of ethanol in the sol-gel to the thickness of the TiO_2 on the optical fiber.

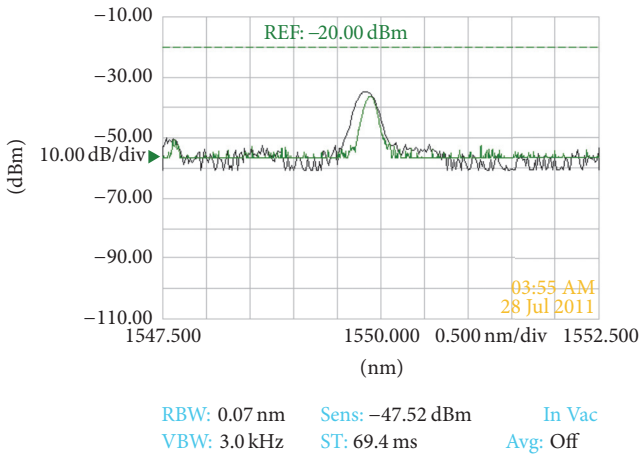

Figure 11: The reflectivity spectrum of the etched-FBG in the air (black line) and the reflectivity spectrum of the same FBG in the deionized water (green line).

5. Conclusion

Higher shifts and narrower peaks in the Bragg wavelength were obtained after coating the fiber with few hundreds nanometers' thick TiO_2 NMO of 20 nm–50 nm hole diameters. The sensitivity of the FBG with the TiO_2 NMO is higher than that without coating due to the nanostructure large surface area. The detected sensitivity was 1.257 nm/riu for air-deionized water and 0.857 nm/riu for air-saline. It is reasonable to be effectively low cost biosensor.

Competing Interests

The authors declare that they have no competing interests.

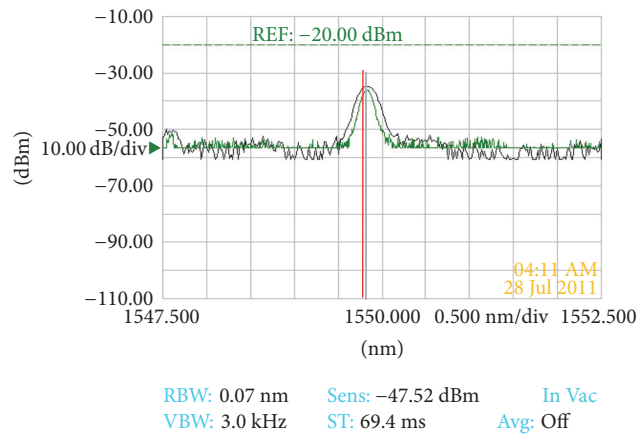

Figure 12: The reflectivity spectrum of the etched-FBG in the air (black line) and the reflectivity spectrum of the same FBG in the saline water (green line).

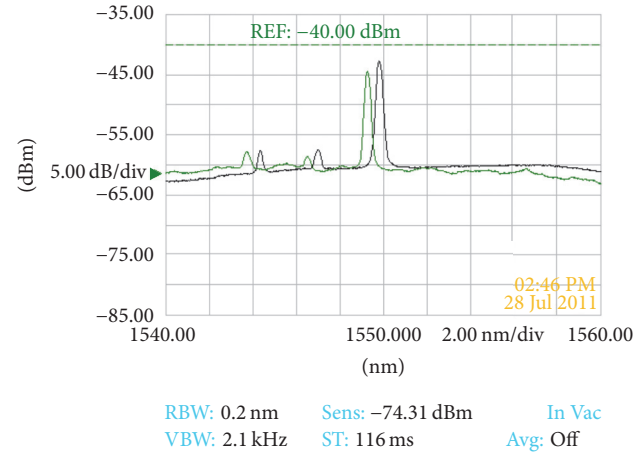

Figure 13: The reflectivity spectrum of the etched-FBG coated with TiO_2 NMO in the air (black line) and the reflectivity spectrum of the same FBG in the deionized water (green line).

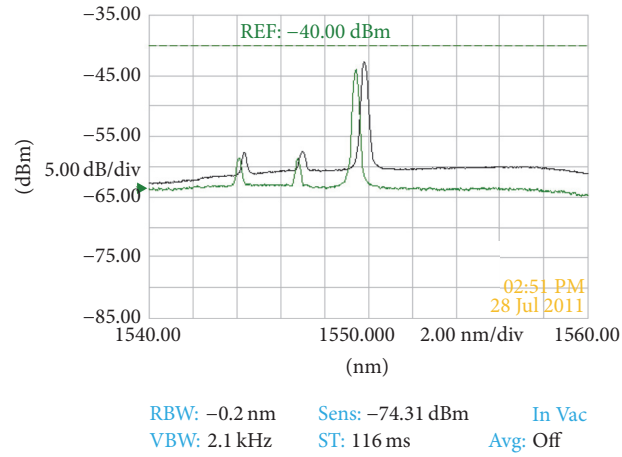

Figure 14: The reflectivity spectrum of the etched-FBG coated with TiO_2 NMO in the air (black line) and the reflectivity spectrum of the same FBG in the saline water (green line).

References

[1] A. Swanton, D. J. Armes, K. J. Young-Smith, C. Dix, and R. Kashyap, "Use of e-beam written, reactive ion etched, phase masks for the generation of novel photorefractive fibre gratings," *Microelectronic Engineering*, vol. 30, no. 1–4, pp. 509–512, 1996.

[2] P. J. Lemaire, R. M. Atkins, V. Mizrahi, and W. A. Reed, "High pressure H_2 loading as a technique for achieving ultrahigh UV photosensitivity and thermal sensitivity in GeO_2 doped optical fibres," *Electronics Letters*, vol. 29, no. 13, pp. 1191–1193, 1993.

[3] K. Zhou, X. Chen, L. Zhang, and I. Bennion, "High-sensitivity optical chemsensor based on etched D-fibre Bragg gratings," *Electronics Letters*, vol. 40, no. 4, pp. 232–234, 2004.

[4] S. Korposh, S.-W. Lee, S. W. James, and R. P. Tatam, "Refractive index sensitivity of fibre-optic long period gratings coated with SiO2 nanoparticle mesoporous thin films," *Measurement Science and Technology*, vol. 22, no. 7, Article ID 075208, 2011.

[5] A. Cusano, P. Pilla, L. Contessa et al., "High-sensitivity optical chemosensor based on coated long-period gratings for sub-ppm chemical detection in water," *Applied Physics Letters*, vol. 87, no. 23, Article ID 234105, pp. 1–3, 2005.

[6] J. F. Akki, A. S. Lalasangi, K. G. Manohar, P. Raikar, T. Srinivas, and U. S. Raikar, "Detection and determination of manganese concentration in water using a fiber Bragg grating coupled with nanotechnology," *Applied Optics*, vol. 50, no. 32, pp. 6033–6038, 2011.

[7] P. T. Arasu, A. S. M. Noor, A. A. Shabaneh et al., "Absorbance properties of gold coated fiber Bragg grating sensor for aqueous ethanol," *Journal of the European Optical Society*, vol. 9, article no. 14018, 2014.

[8] A. G. Mantzila and M. I. Prodromidis, "Development and study of anodic Ti/TiO_2 electrodes and their potential use as impedimetric immunosensors," *Electrochimica Acta*, vol. 51, no. 17, pp. 3537–3542, 2006.

[9] P. R. Solanki, A. Kaushik, V. V. Agrawal, and B. D. Malhotra, "Nanostructured metal oxide-based biosensors," *NPG Asia Materials*, vol. 3, no. 1, pp. 17–24, 2011.

[10] Z. L. Poole, P. Ohodnicki, R. Chen, Y. Lin, and K. P. Chen, "Engineering metal oxide nanostructures for the fiber optic sensor platform," *Optics Express*, vol. 22, no. 3, pp. 2665–2674, 2014.

[11] E. Davies, R. Viitala, M. Salomäki, S. Areva, L. Zhang, and I. Bennion, "Sol–gel derived coating applied to long-period gratings for enhanced refractive index sensing properties," *Journal of Optics A: Pure and Applied Optics*, vol. 11, no. 1, 2009.

[12] K.-S. Mun, S. D. Alvarez, W.-Y. Choi, and M. J. Sailor, "A stable, label-free optical interferometric biosensor based on TiO_2 nanotube arrays," *ACS Nano*, vol. 4, no. 4, pp. 2070–2076, 2010.

[13] R. Liang, Q. Sun, J. Wo, and D. Liu, "Theoretical investigation on refractive index sensor based on Bragg grating in micro/nanofiber," in *Proceedings of the Symposium on Photonics and Optoelectronics (SOPO '11)*, Wuhan, China, May 2011.

[14] M. Smietana, W. J. Bock, and P. Mikulic, "Temperature sensitivity of silicon nitride nanocoated long-period gratings working in various surrounding media," *Measurement Science and Technology*, vol. 22, no. 11, Article ID 115203, 2011.

[15] T. Chen, *Fiber optic sensors for extreme environments [Ph.D. thesis]*, University of Pittsburgh, Swanson School of Engineering, 2012.

[16] X. Zhang, H. Alemohammad, and E. Toyserkani, "Sensitivity alteration of fiber Bragg grating sensors with additive micro-scale bi-material coatings," *Measurement Science and Technology*, vol. 24, no. 2, 2013.

[17] S. C. M. Ho, L. Ren, H.-N. Li, and G. Song, "A fiber Bragg grating sensor for detection of liquid water in concrete structures," *Smart Materials and Structures*, vol. 22, no. 5, Article ID 055012, 2013.

[18] R. Landauer, "Electrical conductivity in inhomogeneous media," *AIP Conference Proceedings*, vol. 40, pp. 2–45, 1978.

[19] Z. L. Poole, P. Ohodnicki, M. Buric et al., "Block copolymer assisted refractive index engineering of metal oxides for applications in optical sensing," in *Nanophotonic Materials XI*, vol. 9161, San Diego, Calif, USA, August 2014.